Infrasonic Array Observations at I53US of the 2006 Augustine Volcano Eruptions

By: C. R. Wilson, John V. Olson, Curt A. L. Szuberla, Steve McNutt, Guy Tytagt, Geophysical Institute, University of Alaska Fairbanks, and Douglas P. Drob, Naval Research Laboratory

Abstract

The recent January 2006 Augustine eruptions, from the 11th to the 28th, have produced a series of 12 infrasonic signals that were observed at the I53US array at UAF. The eruption times for the signals were provided by the Alaska Volcanic Observatory at UAF using seismic sensors and a Chaparral microphone that are installed on Augustine Island. The bearing and distance of Augustine from I53US are, respectively, 207.8 degrees and 675 km. The analysis of the signals is done with a least-squares detector/estimator that calculates, from the 28 different sensor-pairs in the array, the mean of the cross-correlation maxima (MCCM), the horizontal trace-velocity and the azimuth of arrival of the signal using a sliding-window of 2000 data points. The data were bandpass filtered from 0.03 to 0.10 Hz. The data are digitized at rate of 20 Hz. The average values of the signal parameters for all 12 Augustine signals are as follows: MCCM = 0.85 (STD 0.14), Trace-velocity = 0.346 (STD 0.016) km/sec, Azimuth = 209 (STD 2) deg. The celerity for each signal was calculated using the range 675 km and the individual travel times to I53US. The average celerity for all ten eruption signals was 0.27 (STD 0.02) km/sec. Ray tracing studies, using mean values of the wind speed and temperature profiles (along the path) from NRL, have shown that there was propagation to I53US by both stratospheric and thermospheric ray paths from the volcano.

Introduction

The observation of volcanic signals using infrasound arrays has a long history at UAF. Wilson and Forbes (1969) described volcanic signals from many Alaskan volcanic eruptions using several infrasound arrays in Alaska. They identified the source of the signals by using triangulation from different Alaskan arrays. Wilson, Nichparenko, and Forbes (1966) found evidence for multiple sound channel propagation that produced the sequence of observed volcanic signals. In this report we will discuss the recent infrasound observations of signals produced by the eruptions of the Augustine volcano in Alaska during January 2006. During that month the volcano was continuously active and produced several major explosive eruptions. Signals from 12 of the eruptions were observed at I53US at Fairbanks, Alaska.

Augustine Volcano is a 1250-meter-high stratovolcano in southwestern Cook Inlet about 280 km southwest of Anchorage and within about 300 km of more than half of the population of Alaska. Explosive eruptions have occurred seven times since the early 1800s (1812, 1883, 1935, 1964-65, 1976, 1986, and 2006 (Miller et al 1998)). A picture of Augustine is shown in Figure 1below. Following 7 months of increased seismic activity the 2006 Augustine eruptions began with an initial series of vent-clearing explosions sending vertical plumes of volcanic ash up to 10-12 km height that occurred at intervals of a few hours.

15 March 2006 - Inframatics, 18 p.

Figure 1. An aerial photo of Mt. Agustine erupting during January 2006. Photo courtesy of G. McGimsey/USGS

These eruptions occurred on January 11, 13, 14, 17 and again on January 27-28. Each of these explosions was recorded by an on-island Chaparral microphone located 3.2 km east of the volcano crater (station AUE_BDL). See Figure 2 for the AUE_BDL location on the volcano. AUE is the site and BDL is the instrument designator. The zero-to-peak pressure maxima ranged from 14 to 112 Pa at AUE-BDL for the series of explosive eruption signals. AUE_BDL recorded ten explosions that had pressures of 23 Pa or higher, each of which also showed clearly on the Fairbanks infrasound array. An example of an explosion recorded on the local sensor AUE-BDL is shown in Figure 3. On January 28 (23:30 UT) a transitional eruption occurred, marking the onset of phase 2 of the eruption. Phase 2 consisted of small explosions a few minutes apart that produced ash clouds 3-7 km high, and generated pyroclastic flows, surges, block and ash flows and lahars on the volcano flanks. Details of the eruptions and other information about the Augustine volcano can be found at the web site of the Alaska Volcano Observatory (http://www.avo.alaska.edu/).

During the January, 2006 activity period twelve separate infrasound signals were observed at I53US, Fairbanks, Alaska. The great circle distance between Augustine and I53US is approximately 675 km. The signals observed at I53US consisted of wave trains with durations of three to ten minutes with peak-to-peak acoustic amplitudes that ranged from 0.04 to 0.7 Pa. This first period of explosive eruption activity at Mt Augustine was followed after January 29 by non-explosive continuous eruptions phase 2 that did not produce any infrasound signals detected at the Fairbanks infrasound array.

Instrumentation

The Alaska Volcano Observatory operates a series of sensors on Mt. Augustine in order to monitor the volcano's activity. One of those sensors is a Model 2 Chaparral microphone modified to provide a dynamic range that would accommodate the large pressure pulses generated by the volcano during an eruption. The microphone is located at the 'AUE' site on the east flank of the volcano as shown in Figure 2. The presence of acoustic sensors at the volcano makes the combined I53US and AUE data set unique in that we have measurements of the acoustic waveform near the source and at the distant infrasonic array site I53US.

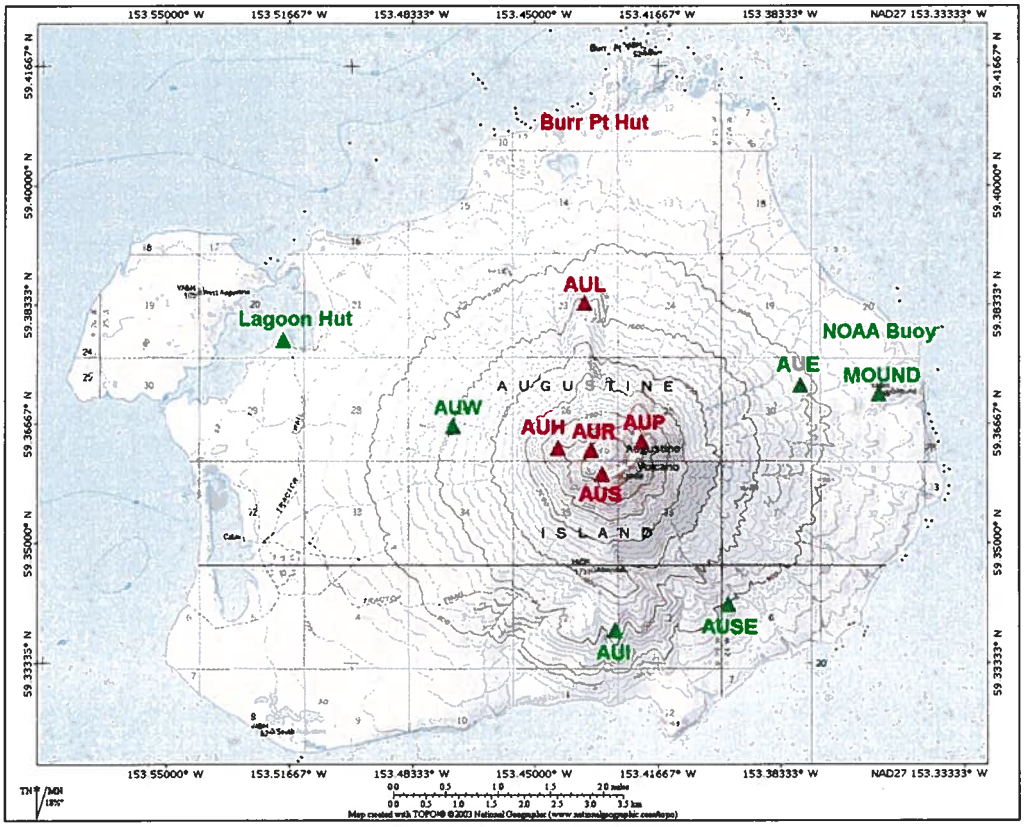

Figure 2. A topographic map of the Augustine volcano showing instrument sites. The infrasound microphone was located on the eastern flank at the site marked AUE, approximately 3.2 km from the peak.

A number of the signals produced by the eruptions of Mt. Augustine were observed at the CTBT/IMS I53US array in Fairbanks, Alaska, nearly 675 km from the volcano. The I53US array is comprised of eight Chaparral model 5 microphones. At I53US there is an outer pentagonal array with aperture 1.7 km of 5 microphones surrounding an inner centered triangular array of three microphones with aperture 0.17 km. The microphone pressure data are digitized at 20 Hz in the CTBTO passband from 0.02 to 10 Hz. The I53US array is located in the forest north of the University of Alaska campus at latitude 64.8671 N and longitude 147.8559 W.

Augustine signals observed at I53US

Table 1 gives a listing of the I53US infrasonic events associated with eruptions on Mt. Augustine during the month of January 2006. There were 12 intervals during which signals from the volcano were observed in the pass band from 0.03 to 0.10 Hz. The signals were associated with volcanic eruptions if their arrival azimuths were consistent with the location of the volcano at 208 deg. and if they also had arrival times that were consistent with the estimated time-of-flight from the volcano to the array. Further, the signals had to have acoustic trace-velocities across the array. The signal detection threshold was set at an MCCM value of 0.5. Excluding the one low-level signal of January 13th (14:02 UT), the average MCCM value for 11 signals was 0.88 with a STD of 0.09. The signal times were determined from the response of the plane-wave estimators of velocity and azimuth and the MCCM correlation values. The details of these determinations are illustrated below in discussions of two representative signals that were received on January 13th (18:25 UT) and 28th (06:09 UT).

Twelve different signals were detected in the pass band from 0.03 to 0.10 Hz, wherein most of the infrasound energy was concentrated. The start and end times for each signal in Table 1 were determined using a least-squares estimator for a plane-wave arrival to give the time series values of MCCM (the mean of the cross-correlation maxima), the trace velocity V and the azimuth of arrival A. The mean value for of the cross-correlation MCCM for all 12 signals listed in Table 1 was 0.85 with a STD of 0.14.

An example is shown in Figure 4 of the least-squares estimator analysis technique for the eruption signal on January 13th (18:25 UT). The azimuth detector plot of A can be seen in the third panel in Figure 4. The detector plot of A can be seen to "lock-on" in the plot at 2.5 minutes to a fixed azimuth of 210 degrees for the duration of the Augustine signal. The true azimuth of the great-circle path from I53US to Augustine is 208 degrees. The signal wavetrain can be seen at the top of Figure 4 as the bestbeam superposition of all 8 sensor pressure traces. The start and end times of the various Augustine signals are thus determined from the time period of the continuous "lock-on" to the correct azimuth for Augustine. The trace-velocity (V) in m/s and the azimuth (A) in degrees are listed in columns 4 and 5 respectively. They are the mean values of Vt and of A over the duration of the signal wavetrains The signal travel time is given in seconds in column 6. These travel times were determined from the eruption time, in column 8, and the signal start time in column 2. The observed signal celerity listed in column 7 is determined for each of the signals by dividing the great-circle range to Augustine of 675 km by the travel time in column 6.The eruption times listed in column 8 for each event were provided by the Alaska Volcanic Observatory at the Geophysical Institute using data from their network of seismometers and the Chaparral microphone on Augustine volcano. The signal RMS pressure amplitude, over the duration of the signal wavetrain, is given in Pa in column11.

Table 1: Augustine Volcano Signal Parameters at I53US

Augustine Volcano eruption signals at I53US Fairbanks, January 2006

data bandpass filtered (0.03 to 0.10 Hz) Propagation path: 2H =2 hop

Date January	signal times start	end	T-Vel m/sec V	Azim deg. A	Signal travel time, Sec	Signal Celerity km/sec from start Time	Eruption time UT	RayPath Strato Celerity km/sec	RayPath Thermo Celerity km/sec	Signal RMS Value Pa
11	14:27:02	14:30:05	337	211.5	2582	0.261	13:44	none	2H, 0.244	0.0361
11	14:56:14	14:58:37	371	213.7	2594	0.26	14:13	none	2H, 0.244	0.0469
13	14:02:23	14:06:34	315	207	2303	0.293	13:24	no profile data		0.0103
13	18:25:00	18:37:16	354	209.8	2280	0.296	17:47	no profile data		0.0269
13	21:02:17	21:12:13	368	209.6	2417	0.281	20:22	2H, 0.299	2H, 0.252	0.0469
14	2:18:30	2:19:30	337	208	2310	0.29	01:40	2H, 0.299	2H, 0.251	0.0169
14	4:45:12	4:50:08	350	211	2832	0.238	03:58	none	2H, 0.246	0.026
14	4:38:32	4:44:22	335	210.7	2432	0.278	03:58	none	2H, 0.246	0.026
14	9:50:57	9:59:00	348	208	2217	0.304	09:14	none	1H, 0.287	0.0642
17	17:43:32	17:52:11	358	208.2	2732	0.247	16:58	none	2H, 0.278	0.0566
28	6:09:22	6:19:26	348	206	2284	0.296	05:31:18	2 H 0.285	1H, 0.284 2H, 0.244	0.0785
28	11:42:39	11:53:46	334	206.7	2293	0.294	11;04;26	2H 0.287	2H, 0.244	0.0796
28	17:27:55	17:35:00	329	208.3	2755	0.245	16:42			0.0362
Average			345.9	209.1						
STD			15.8	2.18						

In order to determine the propagation paths by ray-tracing methods from Augustine to I53US, Doug Drob of the Naval Research Laboratories provided wind- and sound-speed profile data along the great-circle path from the volcano to Fairbanks. This data provided values of sound-speed, wind along the track and wind transverse to the track in three different matrices of size 801 x 609 elements for heights from 0 to 200 km and ranges from 0 to 676 km. For each value of height, from matrix elements 1 to 801, we determined a mean value of sound-speed and the wind component along the track to use in a simple ray-tracing approximation to determine the ray paths for each event. The results of this ray-tracing analysis, using the mean wind and sound-speed at each height level, are displayed in column 9 for stratospheric ray paths and in column 10 for thermospheric ray paths. Appropriate ray paths were selected for which the total distance to the final ray path foot from Augustine, with either one- or two-hop propagation (with reflection at the surface), was within a few kilometers of the 675 km great-circle distance to I53US. Stratospheric propagation ray path results are given in column 9. The word "none" in column 9 means no stratospheric propagation paths were found for that event. The symbol "2H" represents two-hop propagation to I53US. The numerical values in column 9 are the ray path celerities in km/sec for propagation along the ray path from Augustine to I53US. Thermospheric propagation ray path results are given in column10. The numerical values of the ray path celerity for both 1H and 2H paths are given for thermospheric paths in column 10. The calculated ray path travel times from the ray-tracing analysis are used to identify the arrival times for the various modes of propagation of the Augustine signals within the observed wave trains. A detailed discussion will be presented in a later section of the analysis of two Augustine signals for January 13th and 28th. The time of travel (Tp) along each ray path, as well as the angle (Phi) that the ray makes with the surface at its final foot, are determined from ray path analysis for each signal. Using the surface temperature measured at I53US and the ray angle Phi, a "ray-path trace velocity" was calculated for each signal. This calculated trace-velocity was then compared to the observed trace velocity of the signal, as a function of time, along the wavetrain by using the ray path value of Tp.

Atmospheric Fields Model: G2S Fields for the Augustine Event Infrasound Analysis

The Naval Research Laboratory (NRL) Ground to Space (G2S) model (Drob, et al., 2003; Drob, 2004) is used to provide background atmospheric information for the ray trace simulations. The event driven G2S data processing system was used to combine available operational troposphere/stratosphere numerical weather prediction (NWP) specifications from NOAA (Kanamitsu, 1998; Kalnay, et al., 1990) and NASA (Bloom et al., 2005) with the NRLMSISE-00/HWM-93 (Picone et al., 2002, Hedin et al., 1996) upper atmospheric empirical models. This system has spherical harmonic spectral resolution of 121 in the lower atmosphere and incorporates 1° x 1° and 1° x 1.25° resolution global NWP inputs fields to the nearest 6-hour interval. The G2S environmental specifications are provided to the nearest UT hour in order to resolve the upper atmospheric tidal components provided by the NRLMSISE-00/HWM-93 models. At the end of this article we provide several links to model resources.

For each of the 12 events, a series of range dependent profiles is generated along the great circle path from source to receiver to simplify the propagation calculations allowing usage of a 2D, range dependent Cartesian coordinate system. The great circle path is approximated for a spherical earth with an average radius of 6378.206 km. Any deviations from the true great circle path that account for the Earth's oblateness are negligible in the context of the uncertainties of the atmospheric data and the propagation model physics. A total of 609 range steps at 0.01° intervals (~1.1 km) are provided in the horizontal direction, while 801 vertical steps at 0.25 km interval from mean sea level to the thermosphere are given in the vertical direction. These resolutions, which are over sampled relative to in resolution of the input data source, allow for the efficient calculation of range dependent parabolic equation models at a future date. Atmospheric pressure (P) and total mass density (ρ) from the G2S model are used to calculate the static sound speed at all points along the 2D path from the relation $c = \mathrm{sqrt}(\gamma P/\rho)$, where $\gamma = 1.4$. The zonal (u) and meidional (v) wind components from the G2S model were also projected into along track ($u_{||}$) and cross track ($v_{\perp}$) wind components using the relations, $u_{||} = u\cos(\theta) + v\sin(\theta)$ and $v_{\perp} = -u\sin(\theta) + v\cos(\theta)$ with $\theta = 90 - \phi$, where ϕ is the navigational bearing at each point along the propagation path.

Detailed range dependent propagation calculations by a number of researchers have clearly demonstrated that terrain scattering effects should not be ignored in mountainous regions. Therefore, in addition to the atmospheric specifications, terrain elevation estimates at 30" resolution (1 km) are provided along the great circle path with new capabilities built into the G2S system. The NOAA Global Land One-km Base Elevation (GLOBE) digital terrain model provides the underlying data. At 1-km resolution, deviations of the actual elevation along the true great circle path becomes comparable, but again relative to uncertainties in the atmospheric specifications and propagation physics, the general assumptions made to specify the background conditions and lower boundary conditions are reasonable.

The variability of the observed atmospheric conditions over the series of Augustine eruptions provides a unique opportunity to demonstrate the significance of accurate and detailed atmospheric specifications relative to climatology, in order to properly analyze and model infrasound signals. At first glance, the monthly average tropospheric and stratospheric wind conditions for the Alaska region during the time of the events indicate that the wind fields are not very interesting. The source to receiver configuration is poleward enough so as to make the probability of tropospheric ducting by the jet streams very unlikely. Furthermore, the HWM-93 predictions for the peak stratospheric zonal wind velocities are only on the order to 20 to 30 m/s (eastward) as compared to the 60 to 70 m/s (eastward) zonal velocities at mid-latitudes. During this time, however, the stratospheric temperature profiles are such that the peak stratospheric static sound speed approaches or exceeds the static sound speeds at the ground. Under the latter conditions stratospheric ducting will occur in any propagation direction in the absence of winds. This is in contrast to mid-latitudes, where the stratospheric ducting occurs as the result of winds and is directionally dependent.

In addition to the vertical temperature structure, what makes this series of ground-truth events interesting and noteworthy for highlighting the influence to atmospheric conditions and variability on propagation is the fact that stratospheric wind conditions from day-to-day and year-to-year at high-latitudes during winter time can be extremely variable relative to the seasonal average conditions. For example, so much so that during the first eruptions the stratospheric winds during the event were blowing strongly to the south west, so that stratospheric wind component along the propagation path ($u_{||}$) was -40 to -60 m/s, and included a 40 m/s stratospheric cross wind ($v_{\perp}$). Such conditions should totally eliminate the possibility of any stratospheric ducting and result in significant azimuth deviations. The existence and coherence of these large stratospheric wind anomalies conditions on this date was verified in the global NWP input data sources. Several days later these anomalies disappeared locally, with conditions reverting to empirical average-like conditions, having slight eastward wind components making conditions favorable for stratospheric ducting, particularly for the January 13th eruptions. The anomalous westward stratospheric winds return briefly, but at half the magnitude for the January 17th events, only to return again to normal ranges for the January 28th events and conditions possibly favorable for stratospheric ducting. Over the entire series of events there was a slight decrease in both the peak stratospheric and surface temperatures, which mapped to an approximate decrease in static sound speed at both altitudes of about 5 to 10 m/s. Because the ratio of static sound speeds at the two altitudes remained roughly constant, changes in the local and stratospheric wind conditions, as well as local time effects determining the phase of the diurnal and semi-diurnal migrating tides in the lower thermosphere, are likely to be the main cause of any differences in travel times and azimuth deviations observed between the various events. Changes in the ratio of the static sound speed at the ground to the lower thermospheric is also likely to play a significant factor in travel time and azimuth deviation variations.

Observations: January 13, 2006

A large, complex eruption took place on Mt Augustine near 17:47 UT on January 13. Approximately 38 minutes later (approximately 18:25 UT) the beginning of a wave train of signals from the direction of Mt Augustine was detected at I53US. This wave train lasted for about 12 minutes and, we believe, was composed of the arrivals of signals from at least two atmospheric paths.

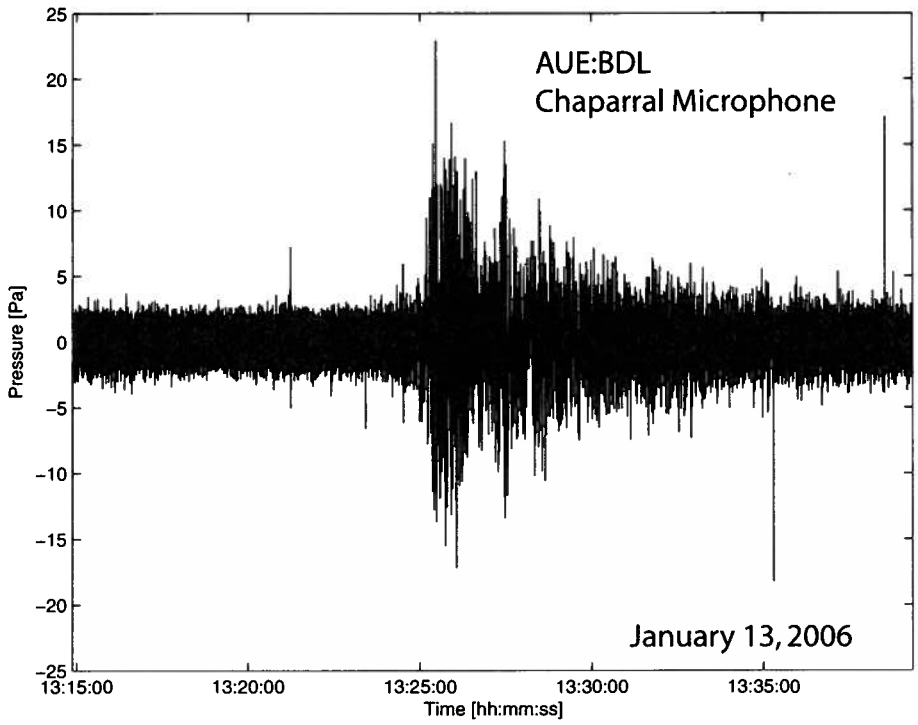

Figure 3. Raw pressure data from the Chaparral microphone located 3.2 km from Augustine volcano. The I53US signal from this 13:25 UT event was observed at 14:02:23 UT, as listed in Table 1.

Figure 4 shows the stacked, phase-delayed signals from I53US formed into a 'best-beam' signal along with estimates of the velocity, azimuth and MCCM[1] correlation-based detector values. The origin time in these plots is 18:20 UT. The raw data were first band-pass filtered between 0.03 and 0.10 Hz to eliminate low frequency, non-acoustic variations and higher-frequency microbarom contamination. Note that as the MCCM values rise above 0.8 near 18:25 UT the velocity and azimuth estimates become steady. The azimuth estimates are very constant at a value of 209 ± 3 degrees, consistent with the expected back azimuth the Augustine. In contrast, the velocity estimates show a trend towards higher values as time progresses. We take this to be due to arrivals from different ray paths as we shall explain below.

In Figure 5 we show the details of the variations of velocity with time. It is clear that there is a trend toward increasing values of trace velocity with time. The least-squares straight line fit is shown in red and has a slope of $2.9*10^{-3}$ (km/s)/min. Waves from Mt. Augustine can arrive at I53US in Fairbanks via two principal paths: stratospheric and thermospheric. The thermospheric paths are longer than the stratospheric paths, so thermospheric signal arrivals should appear later than stratospheric signal arrivals. Further, waves arriving from a thermospheric path will have a steeper angle of incidence with the ground than those from the stratospheric path and therefore show a higher trace

[1] MCCM is the mean of the cross correlation maxima that are computed from all sensor pairs in the array.

velocity. We have investigated these ideas using ray-tracing algorithms with model atmospheric data that represent the atmosphere during this time of year.

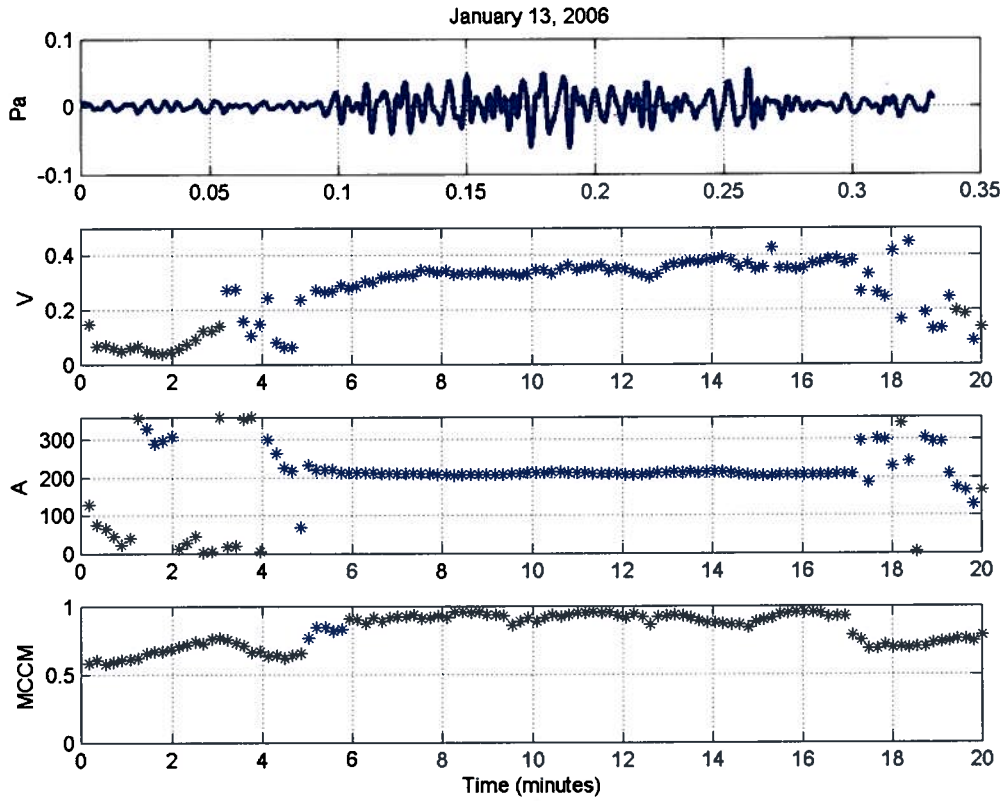

Figure 4. The top panel shows the 'best-beam' waveform derived from the average of the phase-aligned signals from the eight I53US sensors. The second, third and fourth panels show the estimates of velocity, azimuth and MCCM correlation with each point representing averages over a 100 second window. The origin time is at 18:20 UT.

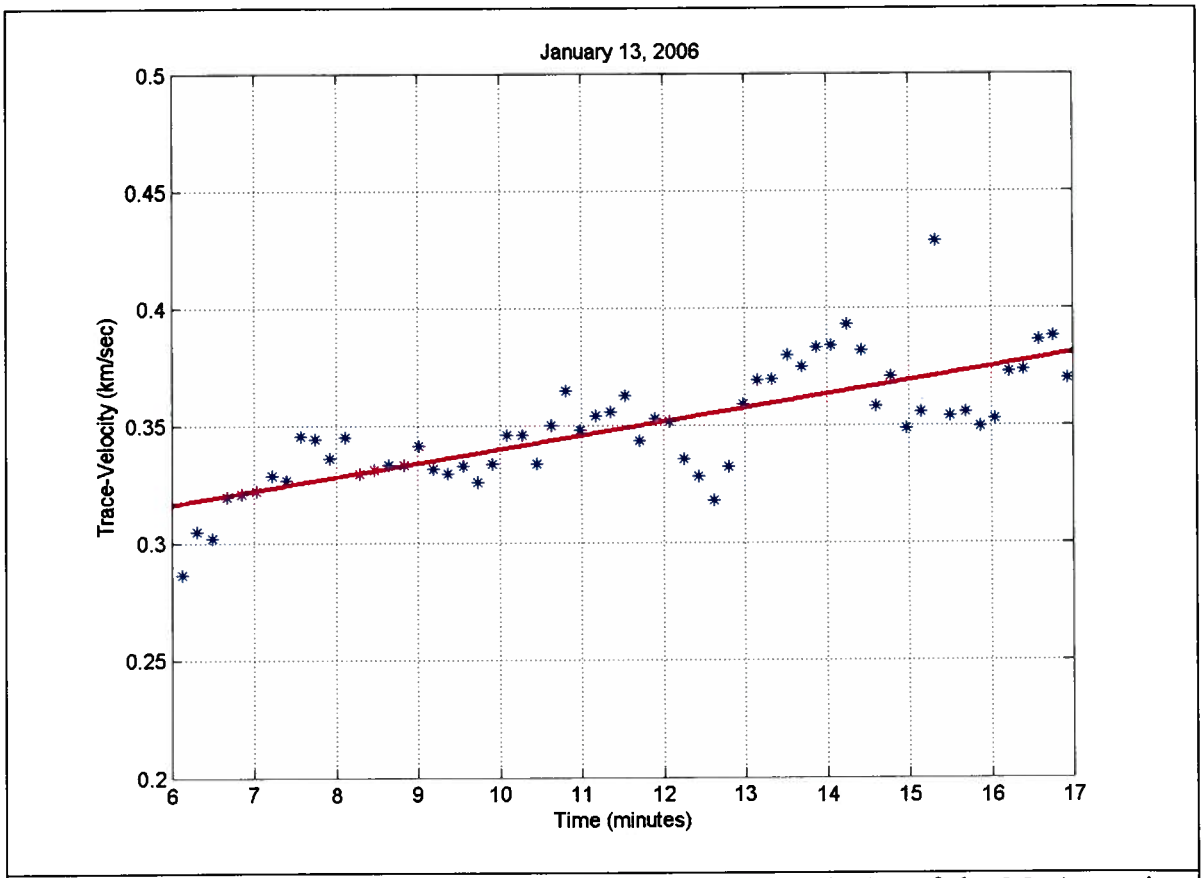

Figure 5. This plot shows the increase in estimated trace-velocity of the Mt Augustine signals across the I53US array as a function of time. The time axis indicates minutes past 18:20 UT. The line is the least squares fit to the data.

Ray Trace Analysis: January 13, 2006

In order to investigate our explanation of the detected velocity increases of the signal with time we have used a ray tracing algorithm in combination with a model atmosphere to estimate time of arrival and angle of incidence of the waves. The model atmosphere was described above and includes the effects of winds along the ray path. For this study we have extracted the mean temperature and mean wind along the ray path from the model atmosphere as input for the ray trace. Rays were investigated with the constraint that a ray would be chosen as representative if it landed within a few kilometers of I53US when launched from Mt. Augustine's peak, at a height of 1.3 km.

The result for the January 13th case is that both the stratospheric and thermospheric ray paths between Augustine volcano and I53US require a bounce midway. Figure 6 shows the ray paths for the January 13th event with the mean temperature and the mean down track winds shown along with the ray path. The two ray paths that connect Mt. Augustine and I53US are shown in the center panel of Figure 6; one involves a stratospheric reflection and the other a thermospheric reflection. The travel times for these two rays are given in Table 2 along with the corresponding celerity. We have also included celerity values, based upon the arrival times taken near the beginning and the

end of the data sequence (see Figure 4). The celerity estimates for each path agree to within 10%. Given that we have used a model atmosphere, with mean temperature and mean wind, along the path, we feel this is good agreement.

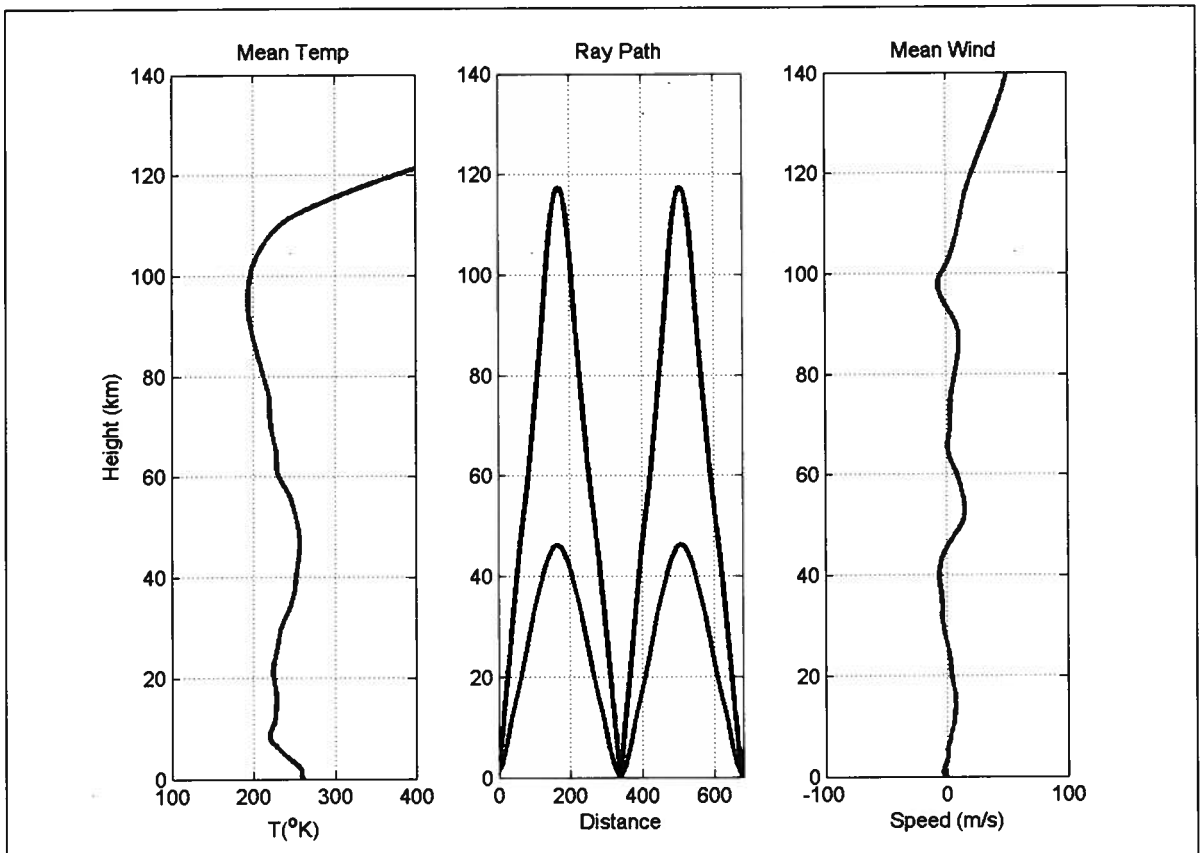

Figure 6. This figure shows the ray paths for the January 13, 2006 events. The left panel shows the mean temperature along the path and the right panel shows the mean wind. The center panel shows the ray paths that connect Augustine and the I53US array.

Table 2: Time-of-Flight, January 13, 2006

Path	Time of flight	Celerity, ray path	Celerity, observed
Stratospheric	2250 seconds	0.297 km/sec	0.288 km/sec (18:27 arrival)
Thermospheric	2670 seconds	0.253 km/sec	0.234 km/sec (18:36 arrival)

Observations: January 28, 2006

Another large eruption took place at Augustine on January 28th (approximately 05:31 UT). Approximately 38 minutes later (06:09 UT) the beginning of a wave train of signals from the direction of Augustine was detected at I53US. This wave train lasted for about

15 minutes and, we believe, was composed of the arrivals of signals from at least two atmospheric paths.

Figure 7 shows the stacked, phase-delayed signals from I53US formed into a 'best-beam' signal along with estimates of the velocity, azimuth and MCCM correlation-based detector values. The time origin in these plots is 06:05 UT. Again, the raw data were first band-pass filtered between 0.03 and 0.10Hz. Note that as the MCCM values rise above 0.8 near 06:08 UT the velocity and azimuth estimates become steady. The azimuth estimates are steady at a value of 209 ± 3 degrees. Again, these azimuths are consistent with what we would expect for Augustine and the velocity estimates show a trend towards higher values as time progresses.

In Figure 8 we show details of the variations of velocity with time. It is clear that there is a trend to increasing values of trace velocity as time proceeds through this event. The least-squares straight line fit is shown in red and has a slope of $1.4*10^{-2}$ (km/s)/min. Again, we have investigated the time-of-flight estimates using ray-tracing algorithms with model atmospheric data that represent the atmosphere during this time of year.

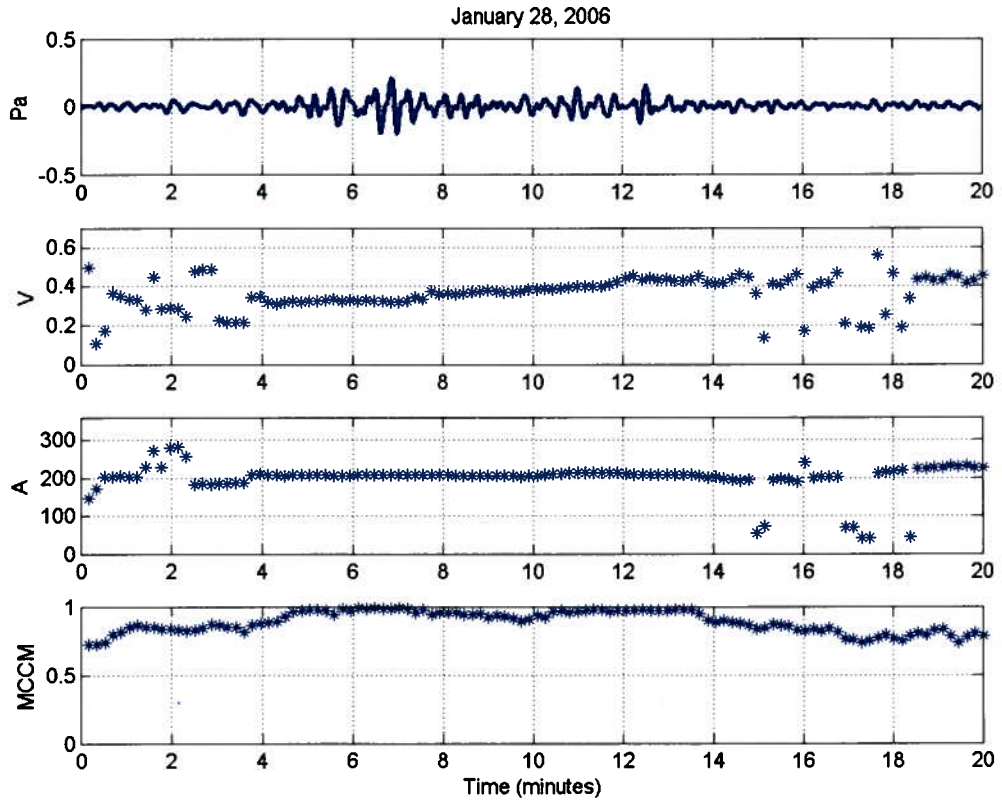

Figure 7. This plot shows the increase in estimated trace-velocity of the Mt Augustine signals across the I53US array as a function of time. The time axis indicates minutes past 06:05 UT

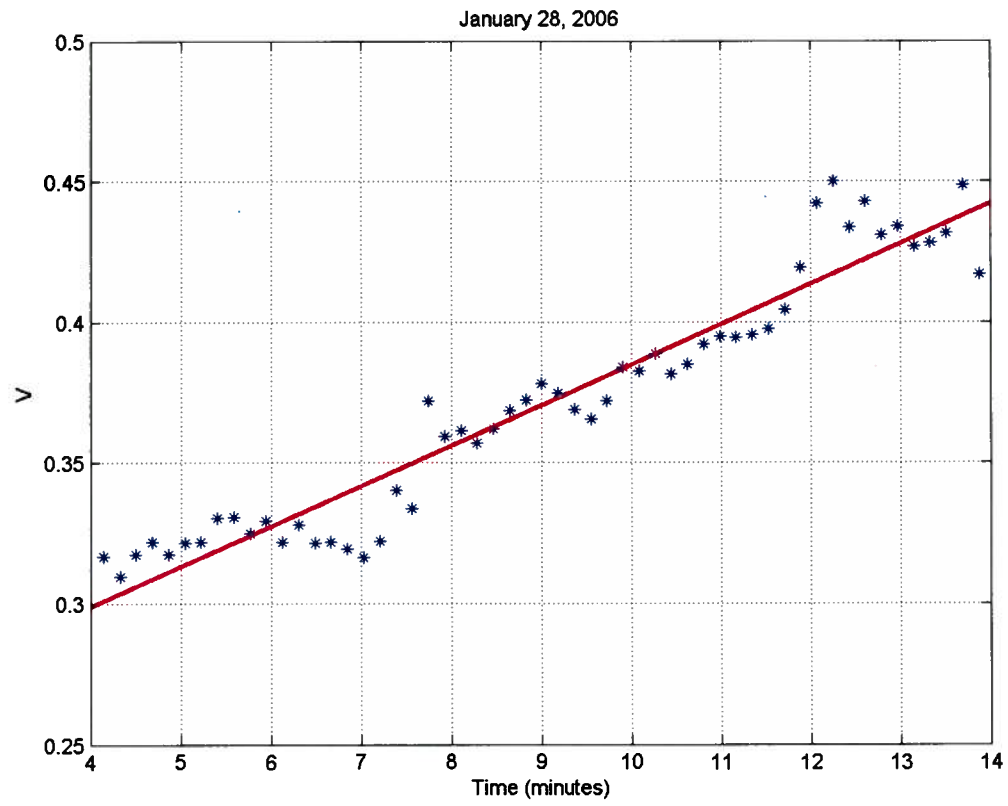

Figure8. This plot shows the increase in estimated trace-velocity of the Augustine signals across the I53US array as a function of time. The time axis indicates minutes past 06:09 UT. The trace-velocity V is in km/sec.

Ray Trace Analysis: January 28, 2006

Again, in order to investigate our explanation of the detected velocity increases of the signal with time we have used a ray tracing algorithm in combination with a model atmosphere to estimate time of arrival and angle of incidence of the waves. For this study we have extracted the mean temperature and mean wind along the ray path from the model atmosphere as input for the ray trace. Rays were investigated with the constraint that a ray would be chosen as representative if it landed within a few kilometers of the I53US array when launched from a 1.3 km altitude, the Augustine volcano summit height.

The result for the January 28th case is that both the stratospheric and thermospheric ray paths between Mt Augustine and I53US require a bounce midway. Figure 9 shows the ray paths for the January 28th event with the mean temperature and mean winds shown along with the ray path. The two ray paths that connect Mt. Augustine and I53US are shown in the center panel of Figure 9; one involves a stratospheric reflection and the other a thermospheric reflection. The travel times for these two rays are given in Table 3 along with the corresponding celerity. We have also included celerity based upon the arrival times taken near the beginning and the end of the data sequence (Figure 8). The

celerity estimates for each path agree to within 5%. Again, we feel this is good agreement based upon the use of a model atmosphere.

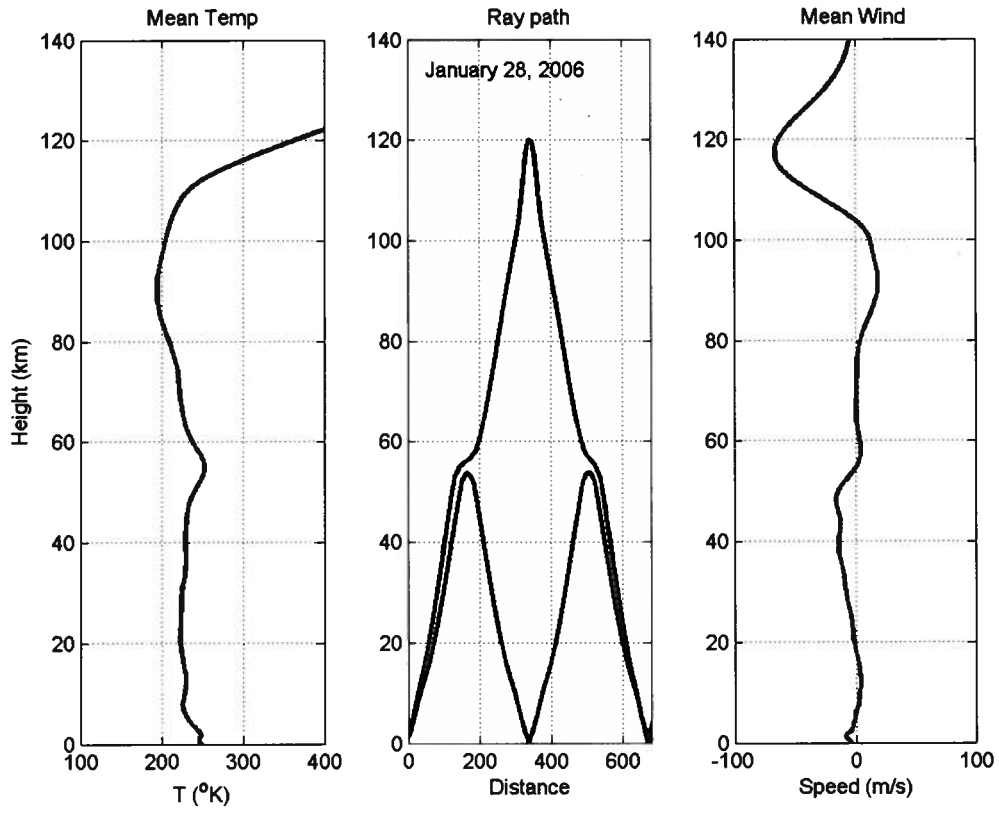

Figure 9. This figure shows the ray paths for the January 28, 2006 events. The left panel shows the mean temperature along the path and the right panel shows the mean wind. The center panel shows the ray paths that connect Mt Augustine and the I53US array.

Table 3: Time-of-Flight, January 28, 2006

Path	Time of flight	Celerity, ray path	Celerity, observed
Stratospheric	2354 seconds	0.285 km/sec	0.298 km/sec (6:09:00 arrival)
Thermospheric (1 hop)	2340 seconds	0.284 km/sec	
Thermospheric (2 hop)	2816 seconds	0.244 km/sec	0.241 km/sec (6.18:00 arrival)

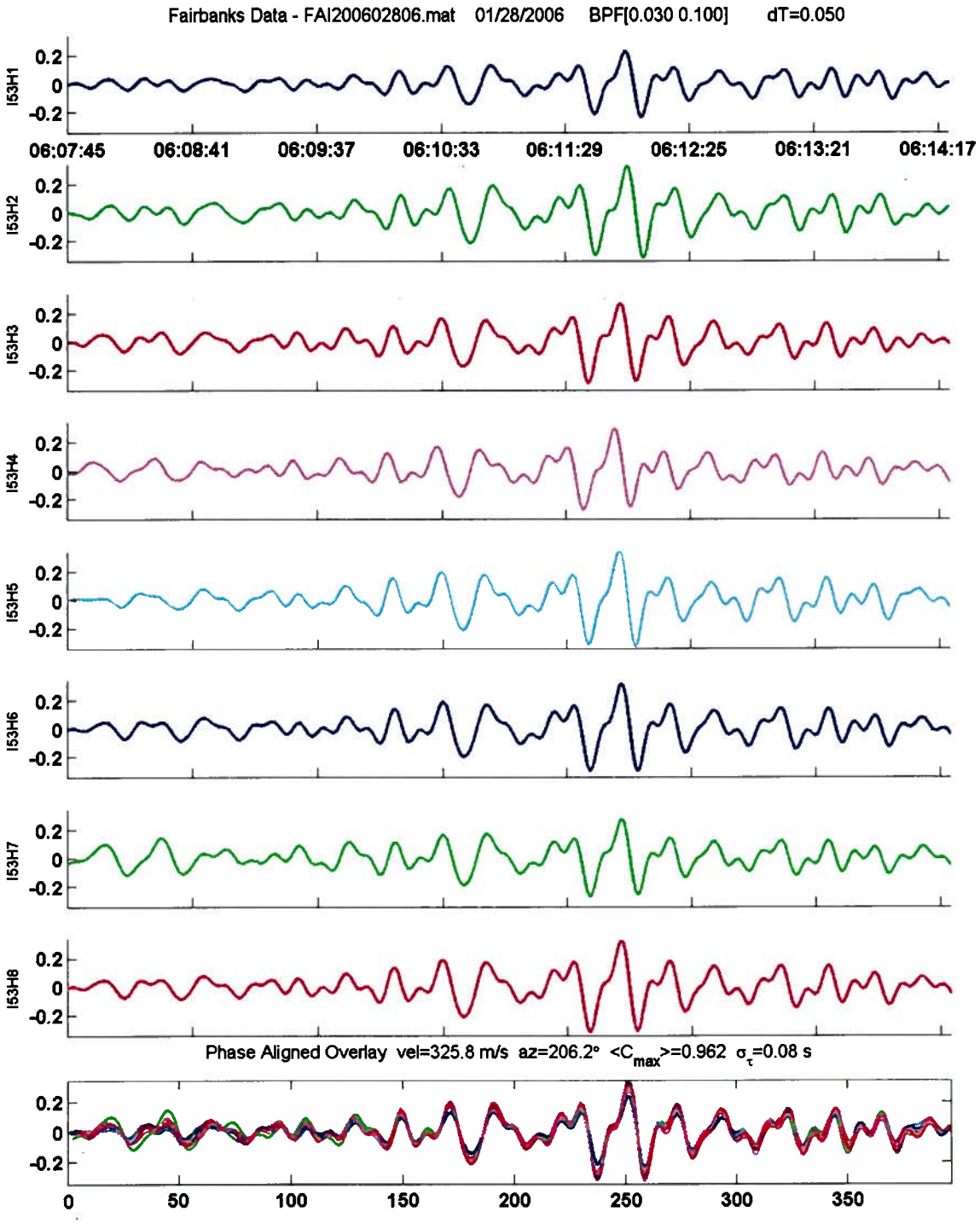

Figure 10. Datascan plot of Augustine eruption signal Jan 28, at 06:09:22 UT With all 8 sensor traces and phase-aligned overlay at the bottom.

In Figure 10 a plot of the January 28th Augustine signal at I53US is shown with all 8 sensor traces and the phase-aligned overlay at the bottom. The obvious similarities in waveform among all 8 sensor traces confirms the high MCCM value that was

determined. This figure is representative of the type of the group of Augustine eruption signals listed in Table1.

Discussion

The variability of the observed atmospheric conditions during the time period of the Augustine eruptions provides an excellent opportunity to demonstrate the significance of accurate and detailed atmospheric specifications relative to the climatology in order to properly analyze and model the infrasound signals by ray tracing methods. The Chaparral microphone located on Augustine itself provides a unique opportunity to compare the amplitude of the infrasonic pressure signal at the source with that at I53US, some 675 km distant. Ray-tracing analysis, using mean wind and temperatures as a first approximation, of the Augustine signals has shown that 2-hop propagation for both stratospheric and thermospheric ray paths can explain the time of arrival of most of the signals listed in Table 1 as were observed at the Fairbanks infrasound array.

Addendum

An additional Augustine signal that was not listed in Table 1 was found in the I53US data set from a fourth eruption on January 28, 2006 that had not previously been seen in the original Augustine signal search. The eruption time was at 08:37 UT and the signal was received at I53US at 09:15:27 with duration of three minutes and 45 seconds. The signal trace- velocity was 0.366 km/sec. The azimuth of arrival was 205 degrees. The peak-to-peak amplitude of this signal was 0.208 Pa. The RMS value for the signal wave train was 0.029 Pa.

References

Bloom, S., A. da Silva, D. Dee, M. Bosilovich, J.-D. Chern, S. Pawson, S. Schubert, M. Sienkiewicz, I. Stajner, W.-W. Tan, M.-L. Wu, Documentation and Validation of the Goddard Earth Observing System (GEOS) Data Assimilation System - Version 4. *Technical Report Series on Global Modeling and Data Assimilation* , NASA/TM-2005-104606, 2005.

Drob, D. P., Atmospheric Specifications for Infrasound Calculations, *InfraMatics Newsletter*, No. 5, March 2004.

Drob, D. P., J. M. Picone, and M. A. Garcés, The Global Morphology of Infrasound Propagation, *J. Geophys. Res.*, *108*, doi:10.1029/2002JD003307, 2003.

Hastings, D. A., and P.K. Dunbar, Development and assessment of the Global Land One-km Base Elevation Digital Elevation Model (GLOBE). *International Society of Photogrammetry and Remote Sensing*, Archives, v. 32, no. 4, pp. 218-221, 1998.

Waythomas, C. F., and Waitt, R. B., 1998, Preliminary volcano-hazard assessment for Augustine Volcano, Alaska: U.S. Geological Survey Open-File Report OF 98-0106, 39 p., 1 plate, scale unknown.

Hedin, A.E., E.L. Fleming, A.H. Manson, F.J. Scmidlin, S.K. Avery, R.R. Clark, S.J. Franke, G.J. Fraser, T. Tsunda, F. Vial, and R.A. Vincent, Empirical Wind Model for the Upper, Middle, and Lower Atmosphere, *J. Atmos. Terr. Phys.*, 58, 1421-1447, 1996.

Kalnay, M. Kanamitsu, and W.E. Baker, 1990: Global numerical weather prediction at the National Meteorological Center. *Bull. Amer. Meteor. Soc.*, 71, 1410-1428.

Kanamitsu, M., Description of the NMC global data assimilation and forecast system. *Wea. and Forecasting*, 4, 335-342., 1989.

Miller T.P., McGimsey R.G., Richter D.H., Riehle J.R., Nye C.I.,Yount M.E., Dumoulin ,Catalog of the historically active volcanoes of Alaska,US Geological Survay Open-FileRep 98-582, 1998

Picone J.M., A.E. Hedin, D.P. Drob, and A.C. Akin, NRLMSISE-00 Empirical model of the atmosphere: statistical comparisons and scientific issues, *J. Geophys. Res.*, 107 (A12): art. no.1468, 2002.

Wilson, C. R., S. Nichparenko and R. B. Forbes, Evidence of two sound channels in the polar atmosphere from infrasonic observations of the eruption of an Alaskan volcano, Nature, **211**, 163, 1966.

Wilson, C. R. and R. B. Forbes, Infrasonic waves from Alaskan volcanic eruptions, J. Geophys. Res., **74**, 4511, 1969.

Web Links for G2S Data Sources

NASA GEOS-4 Analysis - http://gmao.gsfc.nasa.gov/systems/geos4/
NOAA Global Forecast System - http://wwwt.emc.ncep.noaa.gov/gmb/moorthi/gam.html
NOAA GLOBE Digital Terrian Model - http://www.ngdc.noaa.gov/mgg/topo/globe.html